Developmental Cell, Volume *57*

Supplemental information

Transgenerational inheritance of sexual attractiveness via small RNAs enhances evolvability in *C. elegans*

Itai Antoine Toker, Itamar Lev, Yael Mor, Yael Gurevich, Doron Fisher, Leah Houri-Zeevi, Olga Antonova, Hila Doron, Sarit Anava, Hila Gingold, Lilach Hadany, Shai Shaham, and Oded Rechavi

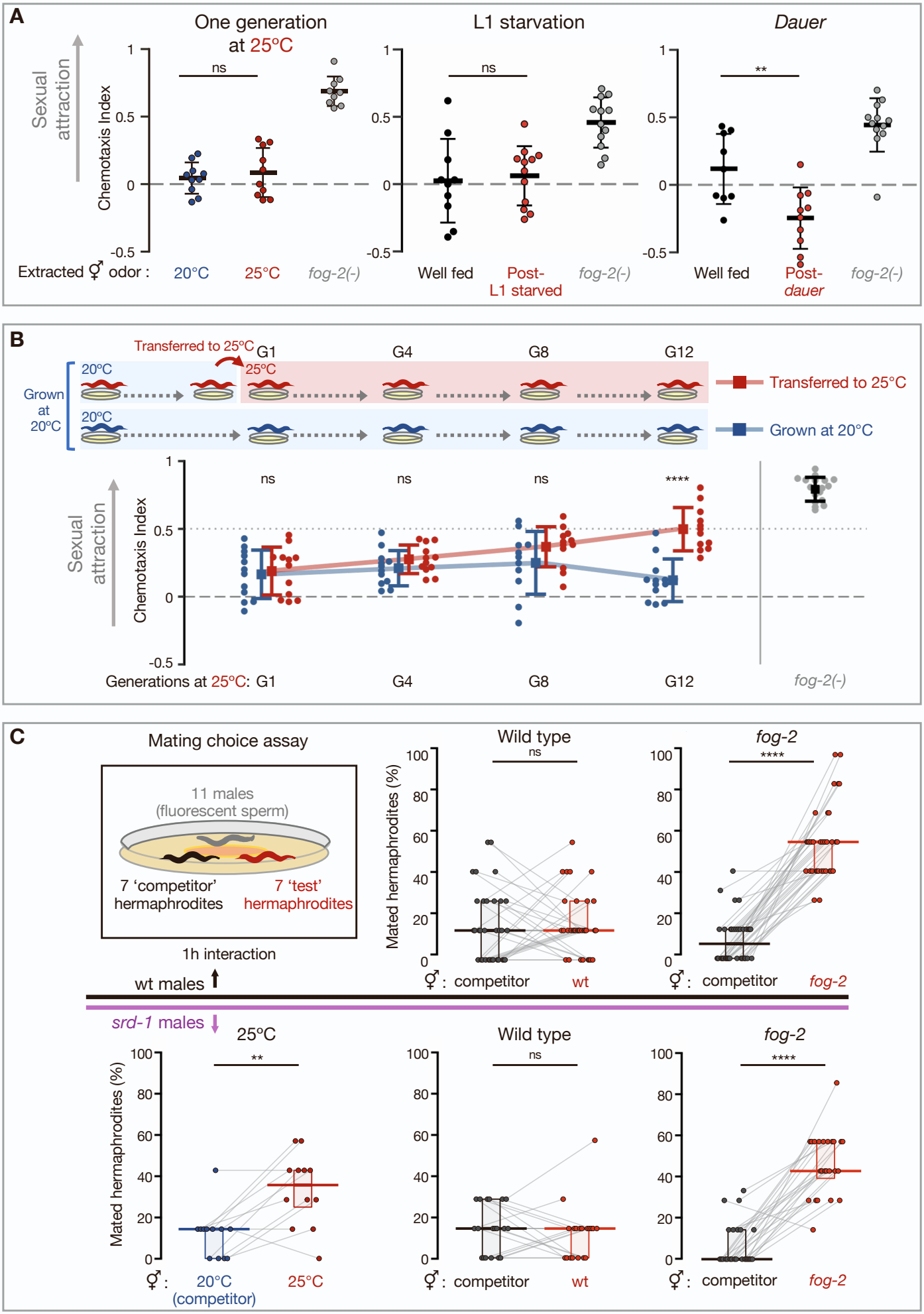
A
One generation at 25°C
L1 starvation
Dauer
Sexual attraction
Chemotaxis Index
ns
ns
**
Extracted ♂ odor :
20°C
25°C
fog-2(-)
Well fed
Post-L1 starved
fog-2(-)
Well fed
Post-dauer
fog-2(-)
B
Transferred to 25°C
G1
G4
G8
G12
Grown at 20°C
20°C
25°C
Transferred to 25°C
Grown at 20°C
Sexual attraction
Chemotaxis Index
ns
ns
ns
****
Generations at 25°C: G1
G4
G8
G12
fog-2(-)
C
Mating choice assay
11 males (fluorescent sperm)
7 'competitor' hermaphrodites
7 'test' hermaphrodites
1h interaction
wt males
srd-1 males
Wild type
fog-2
Mated hermaphrodites (%)
ns
****
♂: competitor
wt
fog-2
25°C
**
20°C (competitor)
25°C

Fig. S1. Examination of premature attractiveness and mating choice among hermaphrodites exposed to different types of environmental stress.
Related to Figure 1.
(A) Male chemotaxis experiments. Tested odorants were extracted from one-day-adult hermaphrodites that were grown at 25ºC (left), that had been starved for 6 days at the L1 larval stage (center) or for 40-45 days in the alternative *dauer* stage (right). One-way ANOVA, Dunnett's correction for multiple comparisons to control. **(B)** Male chemotaxis experiments with odors extracted from hermaphrodites originally grown at 20ºC, transferred to 25ºC and tested after 1, 4, 8 and 12 generations at 25ºC (red). Continuously 20ºC-grown hermaphrodites were used as control (blue). Two-way ANOVA, Sidak's correction for multiple comparisons for every generation. **(A-B)** Each dot represents one biological replicate (chemotaxis plate) with 41-145 wild-type males. Bars: Mean ± sd, results from 3 independent experiments. ****$P < 10^{-4}$, **$P < 0.01$, ns $P > 0.05$. (**C**) Eleven Mitotracker-stained males interacted for exactly one hour with 14 young adult hermaphrodites divided evenly into two groups, "competitor" and "test". In all experiments, the "competitor" hermaphrodites contained an integrated single-copy transgene driving the expression of GFP in the pharynx (strain BFF53). Shown are the proportions (%) of mated hermaphrodites during the 1-hour interaction window, based on the presence of fluorescent sperm in their spermathecae. Experiments were performed using wild-type males (top panel, controls for Fig. 1C) and *srd-1(-)* males (bottom panel). Each grey line represents one biological replicate (mating plate), data collected from at least three independent experiments. Horizontal bar: Median. Boxes: Interquartile range. Two-tailed Wilcoxon matched-pairs signed rank test. ****$P < 10^{-4}$, **$P < 0.01$, ns $P > 0.05$.

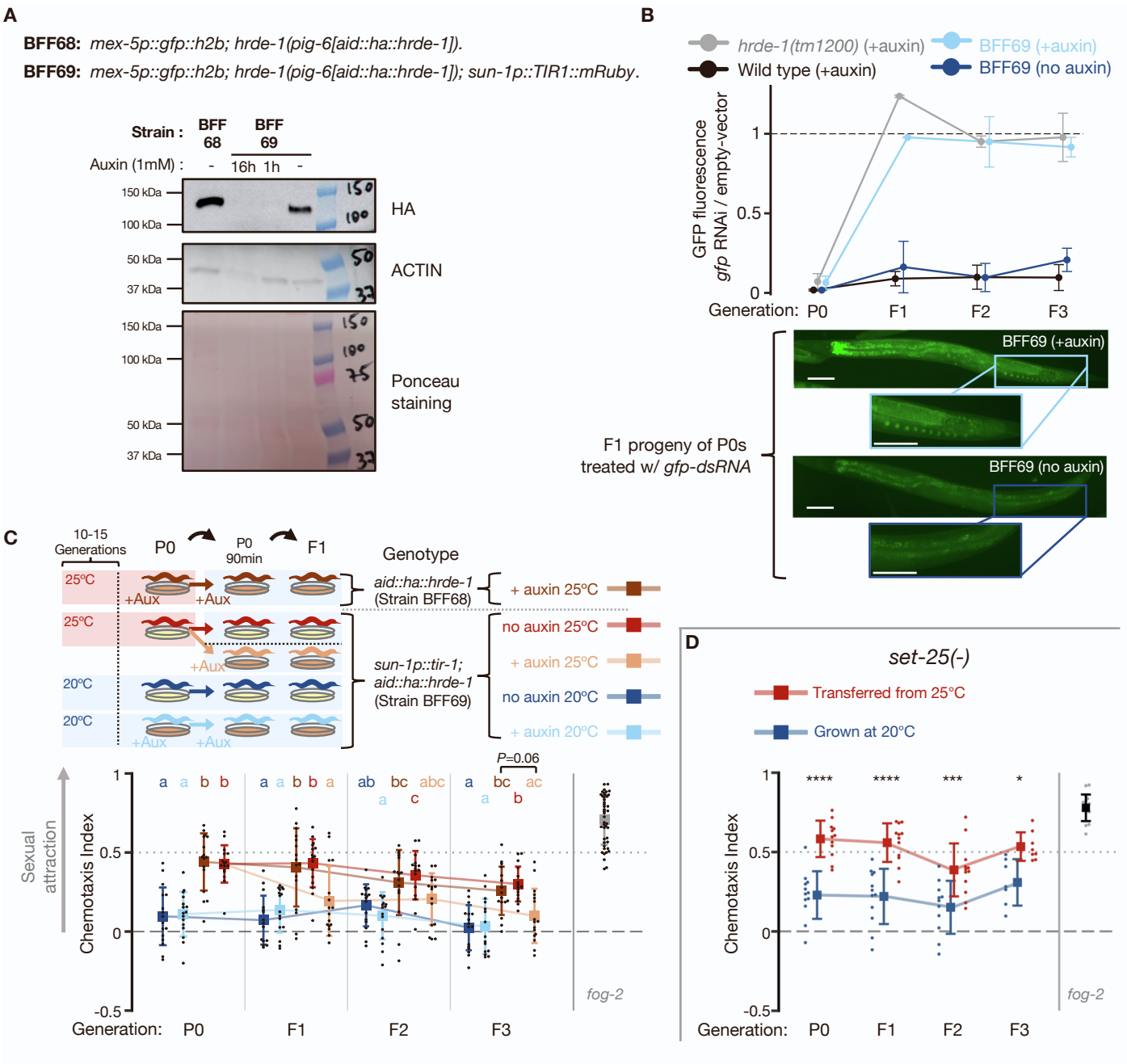

Fig. S2. Conditional knockdown of HRDE-1 using the auxin-inducible degradation (AID) system. Related to Figure 2.

In presence of the plant hormone auxin, the enzyme TIR-1 recognizes proteins containing the 44-amino acid AID tag and send them to degradation (Nishimura et al., 2009; Zhang et al., 2015). Using CRISPR-Cas9, we inserted an *aid::ha* tag at the N' terminus of the endogenous *hrde-1* open reading frame, in worms carrying a single-copy transgene expressing GFP in the germline (BFF68), and subsequently crossed them with worms expressing the TIR-1 enzyme in the germline (BFF69). (**A**) Western blot analysis of lysates extracted from *hrde-1(pig-6[aid::ha::hrde-1])* 1-Day adult hermaphrodites. Strain details and duration of exposure to auxin appear above the images. Membrane was cut horizontally at ~75 kDa. (**B**) (Top panel) - Experiments testing for deficiency in heritable RNAi, the classic phenotype of *hrde-1* knock-out mutants (Buckley et al., 2012). All tested strains contained a single-copy transgene driving the expression of GFP in the germline. To induce a transgenerational RNAi response in the germline, animals were cultivated on plates with bacteria expressing *gfp*-dsRNA (or empty-vector control) for one generation (P0), and transferred to plates with regular bacteria in following generations (F1-F3). GFP fluorescence (y-axis) is depicted relative to the mean fluorescence of control worms of the same genotype exposed to empty-vector control bacteria (at the P0 generation) and imaged side-

by-side. Shown are mean ± sd from two independent experiments. n per group/replicate/generation = 58±14, range 31-88. Bottom panel - Representative images of *gfp* fluorescence in the germline of F1 progeny of *gfp*-RNAi-treated BFF69 worms. Scale bars: 100μm. (**C**) Male chemotaxis experiments with odors extracted from *aid::hrde-1;sun-1p::tir-1* hermaphrodites grown at 25ºC for 10-15 generations (P0) and transferred back to 20ºC for 3 generations in the presence (beige, HRDE-1-depleted) or absence (red) of auxin. The data from Fig. 2 appears again here for convenience of visualization, together with additional control groups. Extraction of odors, and male chemotaxis experiments testing them, were performed side by side for all depicted groups. To ensure HRDE-1 depletion, P0 hermaphrodites were transferred to an intermediate auxin (or control) plate for 90 minutes, before being re-transferred to a new auxin plate where they laid the F1. Control groups included animals continuously grown at 20ºC with (light blue) or without auxin (dark blue), and *aid::hrde-1* animals lacking the *tir-1* gene (BFF68 strain) transferred from 25ºC in the presence of auxin (brown). Each dot represents one biological replicate (chemotaxis plate) with 38-138 males. Bars: mean ± sd, results from 4 independent experiments. Within each generation, data labelled with different letters are significantly different from each other (P<0.05), two-way ANOVA with Tukey's correction for multiple comparisons. (**D**) Male chemotaxis experiments with odors extracted from *set-25(-)* worms grown at 25ºC for 10-15 generations (P0) and transferred back to 20ºC for 3 generations (red), and *set-25(-)* worms continuously grown at 20ºC (blue). Each dot represents one biological replicate (chemotaxis plate) with 43-131 males. Bars: mean ± sd, results from 3 independent experiments, except for the F3 generation (two independent experiments). Two-way ANOVA, Sidak's correction for multiple comparisons for every generation. ****$P < 10^{-4}$, ***$P < 0.001$, *$P < 0.05$.

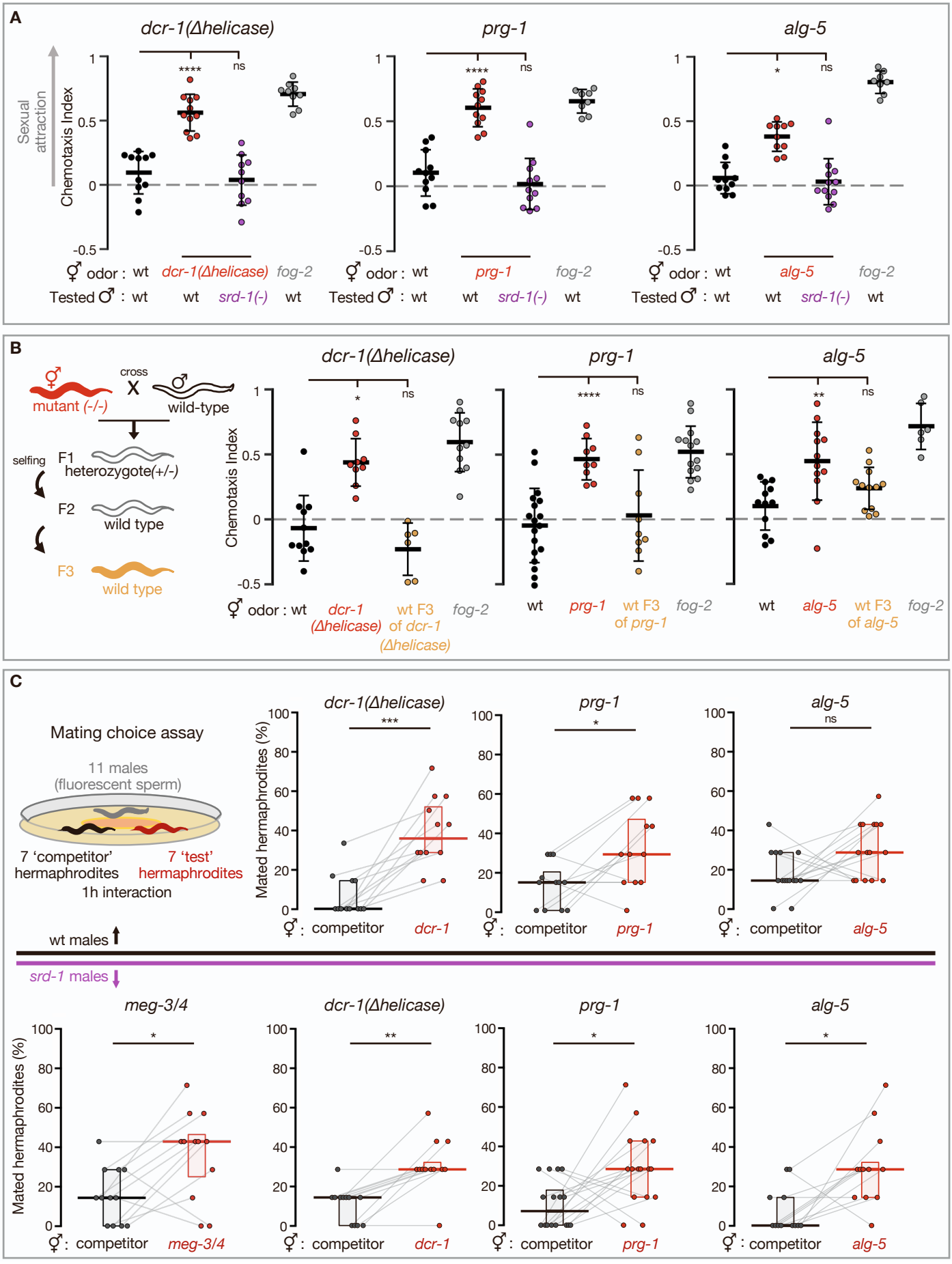
A
dcr-1(Δhelicase)
prg-1
alg-5
Sexual attraction
Chemotaxis Index
1
0.5
0
-0.5
****
ns
*
♂ odor : wt dcr-1(Δhelicase) fog-2
Tested ♂ : wt wt srd-1(-) wt
♂ odor : wt prg-1 fog-2
Tested ♂ : wt wt srd-1(-) wt
♂ odor : wt alg-5 fog-2
Tested ♂ : wt wt srd-1(-) wt
B
mutant (-/-)
cross
X
wild-type
selfing
F1
heterozygote(+/-)
F2
wild type
F3
wild type
dcr-1(Δhelicase)
prg-1
alg-5
Chemotaxis Index
**
♂ odor : wt dcr-1 (Δhelicase) wt F3 of dcr-1 (Δhelicase) fog-2
wt prg-1 wt F3 of prg-1 fog-2
wt alg-5 wt F3 of alg-5 fog-2
C
Mating choice assay
11 males
(fluorescent sperm)
7 'competitor' hermaphrodites
7 'test' hermaphrodites
1h interaction
wt males
srd-1 males
Mated hermaphrodites (%)
100
80
60
40
20
0
***
♂: competitor dcr-1
♂: competitor prg-1
♂: competitor alg-5
meg-3/4
♂: competitor meg-3/4

Fig. S3. Hermaphrodites mutated in small RNA processing genes display premature attractiveness.
Related to Figure 3.
(**A**) Male chemotaxis experiments. Genotypes of hermaphrodites used for odor extraction and of tested males appear below panel. Each dot represents one biological replicate (chemotaxis plate) with 38-163 males. Some of the *alg-5* data appears also in Fig. 3A. One-way ANOVA, Dunnett's correction for multiple comparisons to wild-type (except for *alg-5* panel: Kruskal-Wallis test with Dunn's correction for multiple comparisons to wild-type). Bars: mean ± sd.
(**B**) Male chemotaxis experiments testing for odors extracted from wild-type descendants of *dcr-1(Δhelicase), prg-1* & *alg-5* mutants. Each dot represents one biological replicate (chemotaxis plate) with 38-133 males. One-way ANOVA, Dunnett's correction for multiple comparisons to wild-type (except for *dcr-1(Δhelicase)* panel in [**B**]: Kruskal-Wallis test with Dunn's correction for multiple comparisons to wild-type). Bars: mean ± sd (**C**) Mating choice assays with prematurely attractive small RNA mutants. In all experiments, the "competitor" hermaphrodites had an integrated single-copy transgene driving the expression of GFP in the pharynx (strain BFF53). Shown are the proportions (%) of mated hermaphrodites during the 1-hour interaction window, based on the presence of fluorescent sperm in their spermathecae. Experiments were performed using wild-type males (top panel) and *srd-1(-)* males (bottom panel). Each grey line represents one biological replicate (mating plate), data collected from at least three independent experiments. Horizontal bar: Median. Boxes: Interquartile range. Two-tailed Wilcoxon matched-pairs signed rank test. (**A-C**) ****$P < 10^{-4}$, ***$P < 0.001$, **$P < 0.01$, *$P < 0.05$, ns $P > 0.05$.

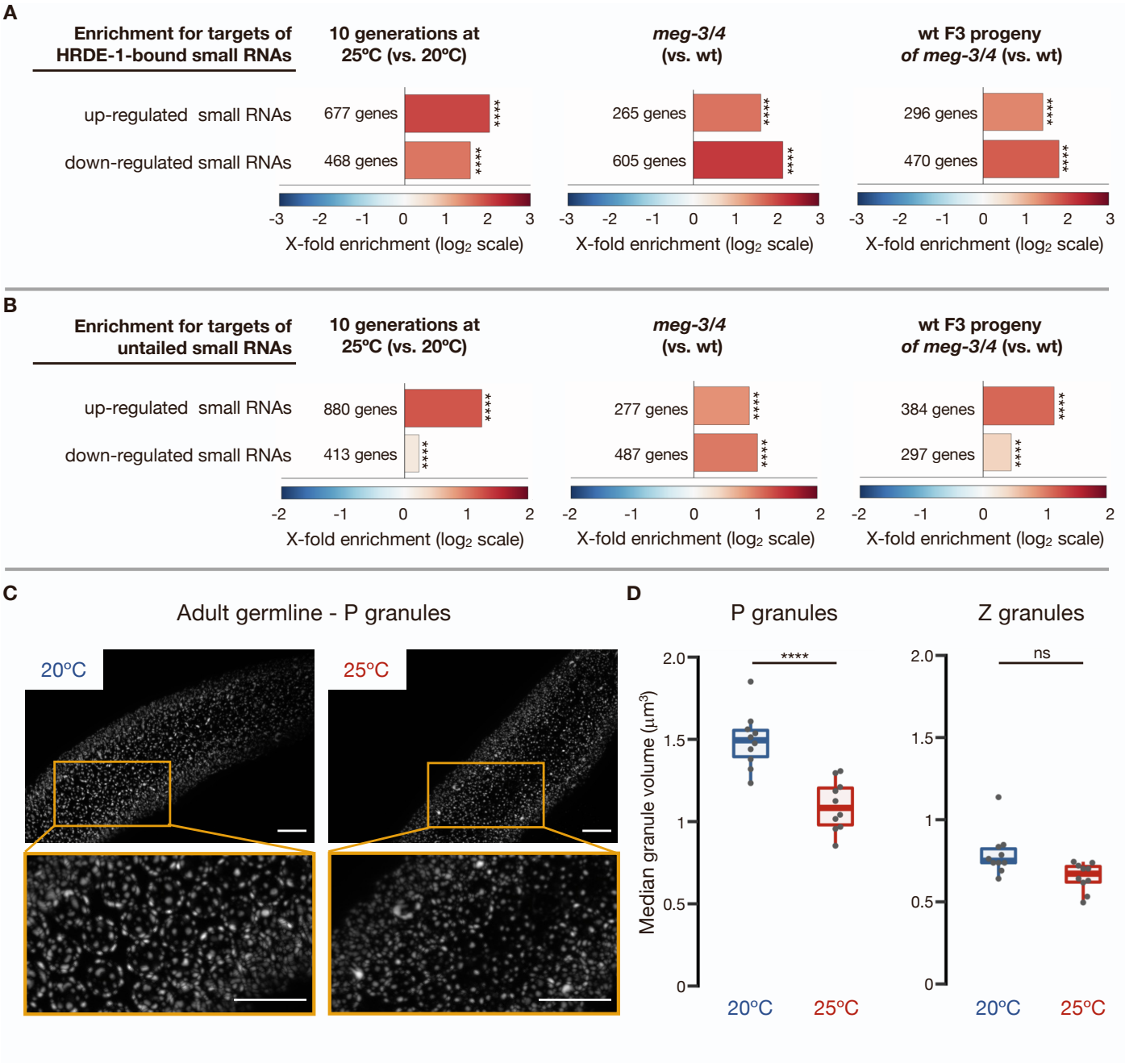

Fig. S4. Premature attractiveness is associated with differential expression of HRDE-1-bound small RNAs and with smaller P granules.
Related to Figure 3.
(A) Enrichment analysis on genes with up-regulated (high bar) and down-regulated (low bar) small RNAs targeting them, in worms that were cultivated at 25ºC for 10 generations (Manage et al., 2020), in long-term *meg-3/4* mutants (<80 generations) (Lev et al., 2019), and in wild-type F3 progeny (two generations of homozygosity) of *meg-3/4* mothers (Lev et al., 2019). Shown are fold enrichment (observed/expected, $\log_2$ scale) in the lists of protein-coding genes targeted by differentially expressed small RNAs, for genes targeted by small RNAs that bind the Argonaute HRDE-1 (Buckley et al., 2012). Differentially expressed small RNAs were analysed with DESeq2, defined by a threshold of adjusted $P < 0.1$. **(B)** Enrichment analysis for genes whose pools of complementary small RNAs contain >90% "untailed" small RNAs, meaning they do not include untemplated 3' Poly-uridyl tails. High proportions of untailed complementary small RNAs is a characteristic of genes targeted by HRDE-1-bound small RNAs (de Albuquerque et al., 2015; van Wolfswinkel et al., 2009). For this analysis, the background list of genes was restricted to gene targets of small RNAs that appeared in the tested experiment (at least 1 RPM), to accommodate the bias in focusing on genes that had poly-U data (see STAR methods). (A + B) *P* values were obtained using a randomization test. (**C-D**) Hermaphrodites grown at 25ºC display

smaller P granules. BFF44 hermaphrodites (N=10 per condition) bearing a *pgl-1::tagRFP* transgene (staining P granules) and a *wago-4::gfp* transgene (Z granules) were imaged as early young adults. (**C**) Representative micrographs of PGL-1::tagRFP fluorescence in the early pachytene zone of hermaphrodites grown at 20ºC (left) and 25ºC for ten generations (right). Scale bars: 10μm. (**D**) Median volume of germ granules in adults grown at 20ºC (blue) and 25ºC for ten generations (red). Each dot represents the median for one individual animal with >1000 analysed granules. Boxplot (Tukey's style): median & IQR, whiskers extend to the most extreme value within 1.5xIQR from the 25th or 75th percentile. One-way ANOVA, Sidak's correction for multiple comparisons. ****$P < 10^{-4}$, ns $P > 0.05$.

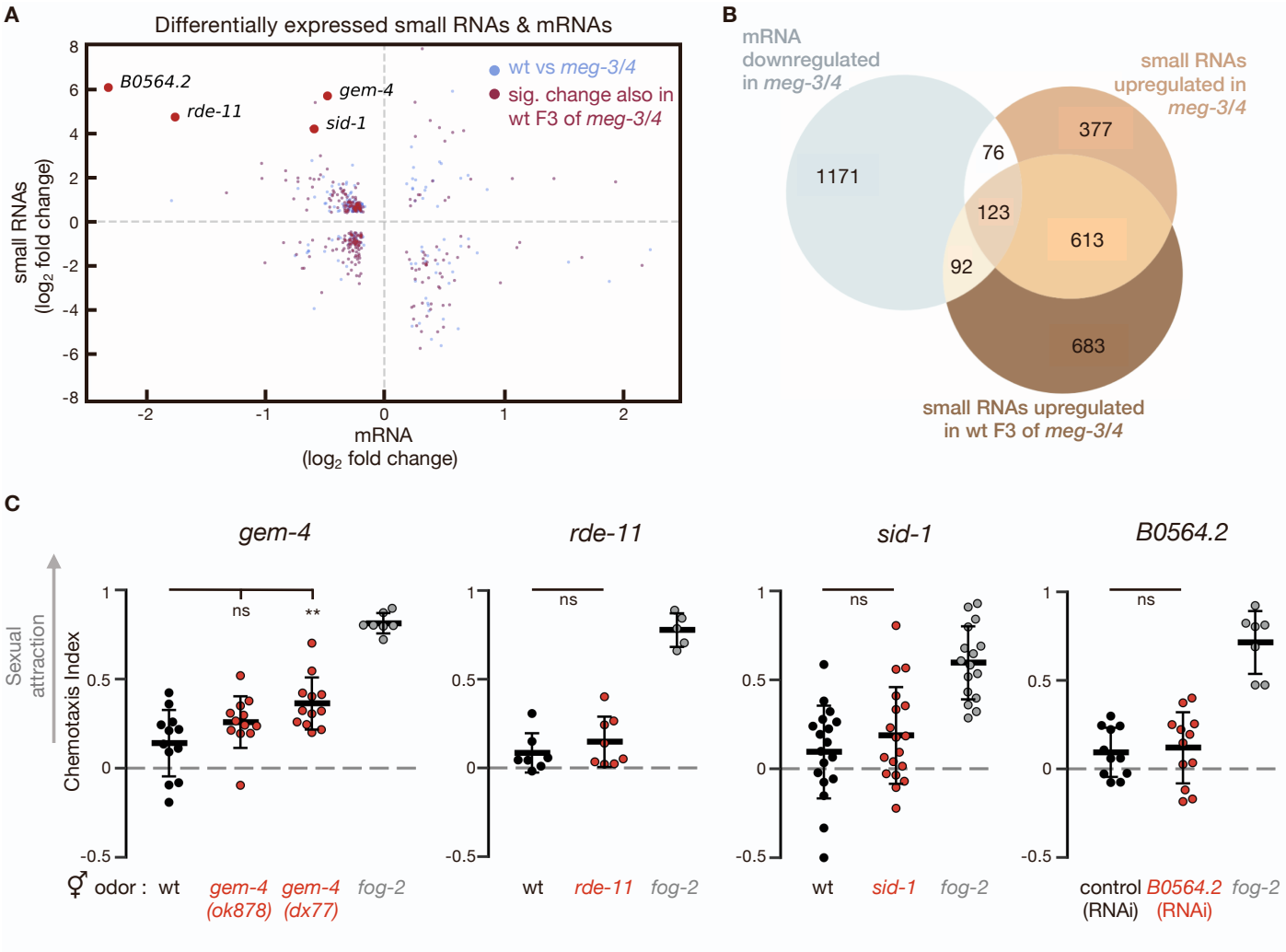

Fig. S5. Examination of candidate genes differentially expressed in wild-type descendants of *meg-3/4* worms.
Related to Figures 3 & 4.
(A) Scatter plot representing genes displaying significant changes in mRNA and small RNA levels (DESeq2, adjusted $P < 0.1$). Sky blue – genes with changes in *meg-3/4* compared to wild-type (small RNA: long-term *meg-3/4* mutants: (Lev et al., 2019) mRNA: (Ouyang et al., 2019)). Red – the subgroup of genes targeted by significantly altered small RNAs also in wild-type F3 progeny (two generations of homozygosity) of *meg-3/4* mutant mothers compared to naïve wild type (Lev et al., 2019). Displayed data for both groups (blue and the red subgroup) represent the changes in the P0 comparison (wt vs *meg-3/4*). **(B)** Venn diagram representing the numbers of genes displaying small RNA and mRNA changes in *meg-3/4* hermaphrodites and in their wild-type F3 progeny, compared to naïve wild type. **(C)** Male chemotaxis experiments. Genotype/condition of hermaphrodites used for odor extraction appears below the panels. Each dot represents one biological replicate (chemotaxis plate) with 43-177 males. The *rde-11* and *sid-1* data appear also in Fig. 3A. One-way ANOVA, Dunnett's correction for multiple comparisons to wild-type. $^{**}P < 0.01$, ns $P > 0.05$.

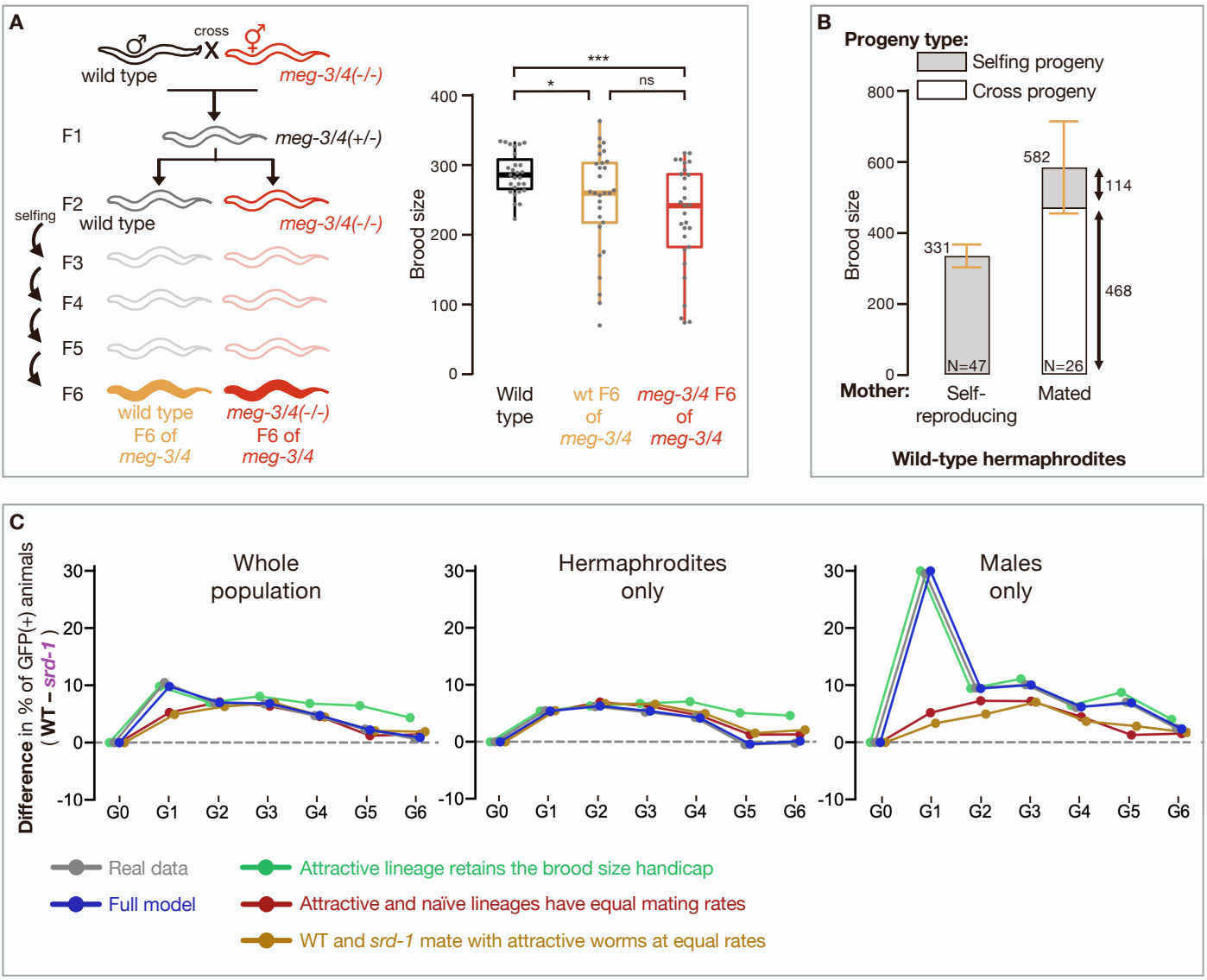

Fig. S6. Additional brood-size analyses and computer simulations related to the multigenerational competition experiment.
Related to Figures 4, 5 & 6.

(**A**) Brood size quantifications of wild-type (black), *meg-3/4* (red) and F6 wild-type descendants of *meg-3/4* hermaphrodites (yellow). As depicted in scheme, *meg-3/4* hermaphrodites were outcrossed with wild-type males, and homozygote F2s were isolated from the cross progeny. F6 descendants from both lineages were used for brood size experiments side by side with wild-type controls. All worms involved contained an integrated single-copy *mex-5p::gfp* transgene in their genetic background. Data collected over 3 independent experiments. Dots represent values for individual hermaphrodites. Boxplot (Tukey's style): median & IQR, whiskers extend to the most extreme value within 1.5xIQR from the 25th or 75th percentile. Welch's ANOVA, Games-Howell post-hoc correction for multiple comparisons. ***P < 0.001, *P < 0.05, ns P > 0.05. (**B**) Brood size quantification of self-reproducing or outcrossed wild-type hermaphrodites, used to generate the theoretical population genetics model (see STAR Methods). Males used for outcrossing contained in their genome an integrated *myo-2p::gfp* transgene (pharyngeal muscles). GFP expression was used to determine mating status of the hermaphrodite and the genetic status of the progeny (selfing-progeny vs. outcrossed progeny). Data collected over 2 independent experiments. Bars: mean ± sd. Rounded averages for total brood size appear near the top left of bars, rounded averages for subgroups appear on the right. Genetic status of progeny is color coded. (**C**) Computer simulations of the multigenerational competition experiment in which different scenarios were tested by relaxing the underlying assumptions of the experiment. Part of the data appears also in Figure 6C and is depicted here for convenience of visualization. On the y-axis is the difference in the proportion of *gfp(+)* worms (attractive lineage) in the population between the wild-type and *srd-1(-)* experiments.

The experimental data from the multigenerational experiment (depicted in Fig. 6B) appear here in grey. The results of the full model (dark blue) reproduce the actual results (grey) with high accuracy. The main null hypothesis assuming equal mating rates for wild type and *srd-1* mutants is depicted in yellow. In this scenario the difference in *gfp(+)*% among males between the two experiments is expected to be substantially lower than the observed experimental results (see right panel). This is also true under the assumption that worms from the attractive lineage (wild-type descendants of *meg-3/4* worms) and the control naïve lineage have the same mating rates (red). We note that in order to accurately recapitulate the experimental results, we had to assume that the epigenetically inherited fitness handicap of the attractive lineage (see panel [A]) is weakened over generations. This assumption is consistent with the transgenerational recovery from RNAi defects witnessed in this lineage (Dodson and Kennedy, 2019; Lev et al., 2019). In contrast, when assuming a constant fitness for the attractive lineage (green), a fairly constant difference between the lineages is observed throughout the generations (middle panel). This deviates from the experimental results where the difference in fitness between the two lineages is substantially reduced by the fifth and six generation.

Genotype	Allele	Chemotaxis index (mean)	Replicates (N)	P value (vs. wt)
Wild type (N2)	—	0.007	32	—
ppw-1	*pk1425*	-0.225	3	0.9999
alg-1	*gk214*	-0.087	4	0.9999
rsd-2	*pk3307*	-0.049	3	0.9999
alg-2	*ok304*	-0.003	4	0.9999
rde-4	*ne299*	0.050	18	0.9999
eri-1	*mg366*	0.051	5	0.9999
hrde-1	*tm1200*	0.070	3	0.9999
rde-11	*hj37*	0.147	8	0.9999
sid-1	*qt9*	0.188	18	0.9318
alg-3/4	*ok1041 ; tm1155*	0.208	3	0.9999
mut-16	*pk710*	0.228	15	0.2379
rrf-3	*pk1426*	0.261	3	0.9999
alg-5	*tm1163*	0.38	10	0.0051
dcr-1(Δhelicase)	*mg375*	0.556	4	0.0077
meg-3/4	*tm4259 ; ax2026*	0.569	3	0.0271
prg-1	*n4357*	0.772	3	0.0018
fog-2	*q71*	0.559	29	$<10^{-4}$

Table S1. Screen of small RNA processing mutants for premature attractiveness. Related to Figure 3.
Information about the results of the screen depicted in Fig. 3A. All odors were extracted from hermaphrodites on the first day of adulthood. The *alg*-5 data appears also in Fig. S3. *P* values were obtained via Kruskal-Wallis test with Dunn's correction for multiple comparisons to wild type.

Parameter	Description	Value
p	Frequency of prematurely attractive worms in the population.	$0 \leq p \leq 1$
m_1, m_2	Mating rate for attractive and nonattractive worms, respectively.	$0 \leq m_1, m_2 \leq 1$
X_c	Brood size (of cross-derived offspring only) for mated hermaphrodites.	450
X_{cs}	Brood size (of selfing-derived offspring only) for mated hermaphrodites.	100
X_s	Brood size for unmated hermaphrodites.	330
f_m	Frequency of spontaneous males.	0.001
	Frequency of males in the progeny of mated hermaphrodites.	0.5
Y_{cmS}	Fitness of cross-derived male, under stress.	1
Y_{cfS}	Fitness of hermaphrodite from crossing, under stress.	$1 - s_m$
Y_{mS}	Fitness of "spontaneous" male, under stress.	$1 - s_c$
Y_{fS}	Fitness of hermaphrodite from selfing, under stress.	$(1 - s_m)(1 - s_c)$
Y_{cm}	Fitness of male from crossing, under no stress.	1
Y_{cf}	Fitness of hermaphrodite from crossing, under no stress.	1
Y_m	Fitness of "spontaneous" male, under no stress.	1
Y_f	Fitness of hermaphrodite from selfing, under no stress.	1
p_m	Fraction of males in the population.	$0 \leq p_m \leq 0.5$
s_m	Male relative fitness advantage under stress.	0.1
s_c	Crossed progeny relative fitness advantage under stress.	0.4
E_S	Likelihood of stress.	0-1
C	Cost of premature attraction.	$0 \leq C \leq 1$
V	Level of premature attraction.	$0 \leq V \leq 1$

Table S4. Parameters used in the mathematical models.
Related to STAR Methods.

Mother	Father	Probability that offspring will be prematurely attractive	Probability to form pairing of this type	Brood size
+	+	1	$p \cdot (m_1 \cdot p)$	X_c
–	+	0.5	$p \cdot m_2 \cdot (1-p)$	X_c
+	–	0.5	$(1-p) \cdot (m_1 \cdot p)$	X_c
+	no father, unmated mothers	1	$p \cdot (1-m_1)$	X_s
+	no father, selfing-derived progeny in mated mothers	1	$p \cdot m_1$	X_{cs}

Table S5. Types of mating events that may produce prematurely attractive offspring. Related to STAR Methods.

In the table, ' + ' signs mark individuals carrying the premature attractiveness trait and ' – ' signs mark all other individuals.